C-terminal acidic domain of histone chaperone human NAP1 is an efficient binding assistant for histone H2A-H2B, but not H3-H4

Hideaki Ohtomo[1], Satoko Akashi[1], Yoshihito Moriwaki[1], Mitsuru Okuwaki[2], Akihisa Osakabe[3], Kyosuke Nagata[2], Hitoshi Kurumizaka[3] and Yoshifumi Nishimura[1]*

[1]*Graduate School of Medical Life Science, Yokohama City University, 1-7-29 Suehiro-cho, Tsurumi-ku, Yokohama 230-0045, Japan*
[2]*Faculty of Medicine and Graduate School of Comprehensive Human Sciences, University of Tsukuba, 1-1-1 Tennodai, Tsukuba 305-8575, Japan*
[3]*Graduate School of Advanced Science and Engineering/RISE, Waseda University, 2-2 Wakamatsu-cho, Shinjuku-ku, Tokyo 162-8480, Japan*

Nucleosome assembly protein 1 (NAP1) binds both the $(H3–H4)_2$ tetramer and two H2A–H2B dimers, mediating their sequential deposition on DNA. NAP1 contains a C-terminal acidic domain (CTAD) and a core domain that promotes dimer formation. Here, we have investigated the roles of the core domain and CTAD of human NAP1 in binding to H2A–H2B and H3–H4 by isothermal calorimetry and native mass spectrometry and compared them with the roles of yeast NAP1. We show that the hNAP1 and yNAP1 dimers bind H2A–H2B by two different modes: a strong endothermic interaction and a weak exothermic interaction. A mutant hNAP1, but not yNAP1, dimer lacking CTAD loses the exothermic interaction and shows greatly reduced H2A–H2B binding activity. The isolated CTAD of hNAP1 binds H2A–H2B only exothermically with relatively stronger binding as compared with the exothermic interaction observed for the full-length hNAP1 dimer. Thus, the two CTADs in the hNAP1 dimer seem to provide binding assistance for the strong endothermic interaction of the core domain with H2A–H2B. By contrast, in the relatively weaker binding of hNAP1 to H3–H4 as compared with yNAP1, CTAD of hNAP1 has no significant role. To our knowledge, this is the first distinct role identified for the hNAP1 CTAD.

Introduction

In eukaryotes, DNA is stably stored in the highly ordered structure, chromatin. The fundamental repeating structural unit within chromatin is the nucleosome, which comprises approximately 146 bp of DNA wrapped around a histone octamer, consisting of two dimers of H2A–H2B and one tetramer of $(H3–H4)_2$ (Luger 2003). The nucleosome is assembled in a stepwise manner: First, the $(H3–H4)_2$ tetramer is deposited onto DNA, and then, two heterodimers of H2A–H2B are added to complete the nucleosome (Akey & Luger 2003). Histone chaperones are necessary for assembly and disassembly of the nucleosome and therefore play important roles in several cellular processes such as chromatin remodeling, cell cycle control, DNA replication and transcription (De Koning et al. 2007; Eitoku et al. 2008).

Nucleosome assembly protein 1 (NAP1) was originally identified from HeLa cell extracts (Ishimi et al. 1984) as a factor mediating nucleosome assembly in vitro. Several lines of evidence have suggested that NAP1 in cooperation with the histone acetyltransferase CBP/p300 regulates the gene expression program by changing chromatin structure (Shikama et al. 2000; Asahara et al. 2002; Luebben et al. 2010); however, it is currently unclear how NAP1 brings about these changes. NAP1 is highly conserved from human to yeast, and the biochemical activities of NAP1 as a histone chaperone have been extensively characterized using the yeast NAP1 (yNAP1) protein.

yNAP1 binds strongly to both the (H3–H4)$_2$ tetramer and two H2A–H2B dimers *in vitro* with Kd values of approximately 10 nM (Andrews *et al.* 2010) and mediates their sequential deposition on DNA. NAP1 also disassembles nucleosomes by removing H2A–H2B in an ATP-independent manner (Ito *et al.* 2000; Park *et al.* 2005; Kimura *et al.* 2006). When mixed with the ATP-dependent remodeling factor, RSC, yNAP1 mediates the complete removal of histones from nucleosomes (Lorch *et al.* 2006). In addition, yNAP1 binds to H2A.Z–H2B and replaces H2A–H2B in nucleosomes with H2A.Z–H2B (Mizuguchi *et al.* 2004; Park *et al.* 2005). Furthermore, thermodynamic analyses have shown that yNAP1 promotes nucleosome assembly by preventing random binding of H2A–H2B to DNA (Andrews *et al.* 2010).

NAP1 proteins form homo- and heterodimers through the conserved central region (Park & Luger 2006; Attia *et al.* 2011), and the arch-like shaped yNAP1 dimer is suggested to bind histones using the acidic surface of the dimer (D'Arcy *et al.* 2013). However, the solution structure of yNAP1 is complicated; under high salt conditions, yNAP1 predominantly exists as a dimer, whereas under physiological salt conditions, it forms multimers including dimers, tetramers, octamers and hexadecamers (McBryant & Peersen 2004; Toth *et al.* 2005; Noda *et al.* 2011; Bowman *et al.* 2014). In addition, the exact binding stoichiometry of yNAP1 to H2A–H2B seems to be controversial because yNAP1 dimer has been shown to bind either one (Toth *et al.* 2005) or two (D'Arcy *et al.* 2013) H2A–H2B heterodimers. *Xenopus laevis* NAP1 (xNAP1) has also been found to form multimers with histones H2A–H2B and H3–H4 at a stoichiometry of one xNAP1 dimer to one histone fold dimer (Newman *et al.* 2012).

The C-terminal acidic domain (CTAD) of NAP1 was shown to contribute to its stable histone binding (Andrews *et al.* 2008) and to the eviction of H2A–H2B dimers from the nucleosome (Park *et al.* 2005; Park & Luger 2006); however, yNAP1 CTAD is not required for nucleosome assembly (Fujii–Nakata *et al.* 1992; Park & Luger 2006). We have previously shown that a CTAD deletion mutant of hNAP1 showed significantly lower nucleosome assembly activity than wild type, indicating that the mechanisms underlying the histone binding and nucleosome assembly of hNAP1 are different from those of yNAP1 (Okuwaki *et al.* 2010). Although hNAP1 shows both histone binding and nucleosome assembly activities similar to yNAP1, its biochemical parameters for histone binding and preference for H2A–H2B

dimers or (H3–H4)$_2$ tetramers, and stoichiometry of histone binding remain elusive.

Here, we have investigated the roles of the core domain and CTAD of hNAP1 in binding to H2A–H2B and H3–H4 by isothermal calorimetry (ITC) and native mass spectrometry (MS) (Benesch *et al.* 2007; Heck 2008; Azegami *et al.* 2013) and compared them with the roles of yNAP1. We show that hNAP1 and yNAP1 dimers strongly and sequentially bind two H2A–H2B heterodimers as first and second H2A–H2B heterodimers by two different modes: exothermically and endothermically. Notably, an hNAP1 mutant lacking CTAD weakly binds a single H2A–H2B heterodimer and then partially binds a nonstabilized H2A–H2B heterodimer only by the endothermic mode, whereas the corresponding yNAP1 mutant strongly and sequentially binds two H2A–H2B heterodimers by the two different modes, similar to full-length yNAP1. In addition, the isolated CTAD of hNAP1, but not the yNAP1 CTAD, can bind to a single H2A–H2B heterodimer exothermically. This suggests that the CTADs of hNAP1, but not those of yNAP1, act as a binding assistant for H2A–H2B. In contrast, the hNAP1 dimer binds single and double H3–H4 heterodimers without the contribution of the CTADs.

Results

hNAP1 uses two modes to interact with H2A–H2B, but a single mode to interact with H3–H4

We prepared full-length hNAP1 (hNAP1^{FL}, amino acids 1–391), a CTAD deletion mutant (hNAP1ΔC, amino acids 1–344), an N-terminal deletion mutant (hNAP1ΔN, amino acids 49–391) and the isolated CTAD (amino acids 349–381). ITC experiments showed that hNAP1^{FL} bound H2A–H2B by two different modes, endothermically (heat absorption) and exothermically (heat release) (Fig. 1A). The Kd value of the endothermic interaction was approximately 10 nM, whereas that of the exothermic interaction was over 1000 nM (Table 1); thus, the endothermic interaction seems to be the essential mode of binding between hNAP1 and H2A–H2B. Similar to hNAP1^{FL}, hNAP1ΔN bound strongly to H2A–H2B by exothermic and endothermic binding modes (Fig. 1B). In contrast, hNAP1ΔC lost the exothermic interaction and showed greatly reduced H2A–H2B binding activity with a Kd value for the endothermic interaction of approximately 300 nM (Fig. 1C, Table 1). Thus, the two CTADs in the hNAP1

dimer contribute to exothermic binding to H2A-H2B and also enhance the endothermic binding of the core domain. In fact, the isolated CTAD bound H2A-H2B only exothermically (Fig. 1D), although the Kd value of 80 nM indicated relatively stronger binding as compared with the exothermic interaction observed for hNAP1[FL]. Thus, both CTADs in the hNAP1 dimer seem to act cooperatively to provide binding assistance for the endothermic interaction of the core domain.

Similarly, yNAP1 (yNAP1[FL], amino acids 1–417) bound to H2A-H2B by exothermic and endothermic modes (Fig. S1 and Table S1 in Supporting Information); however, a yNAP1 mutant lacking CTAD (yNAP1ΔC, amino acids 1–365) still showed both binding modes to H2A-H2B with binding activities similar to those of the full-length protein. In the case

of yNAP1, maybe because of its equilibrium between oligomers, a quantitative estimation of Kd values was difficult from the present ITC curves; however, both binding curves seemed to be similar, suggesting that the CTAD of yNAP1 does not play a significant role in binding to H2A-H2B. This corresponds well with previous studies, which showed that the binding activity of yNAP1 to H2A-H2B remained similar after deletion of the CTAD (Andrews *et al.* 2008).

Similarly, yNAP1 showed strong binding to H3-H4 by exothermic and endothermic modes (Fig. S1 and Table S1 in Supporting Information). It has been well established that yNAP1 binds strongly to H3-H4 with a Kd value of approximately 10 nM similar to that for H2A-H2B binding (Andrews *et al.* 2010). In contrast, hNAP1 bound H3-H4 only endothermically with a Kd value of approximately 200 nM (Fig. 1E,
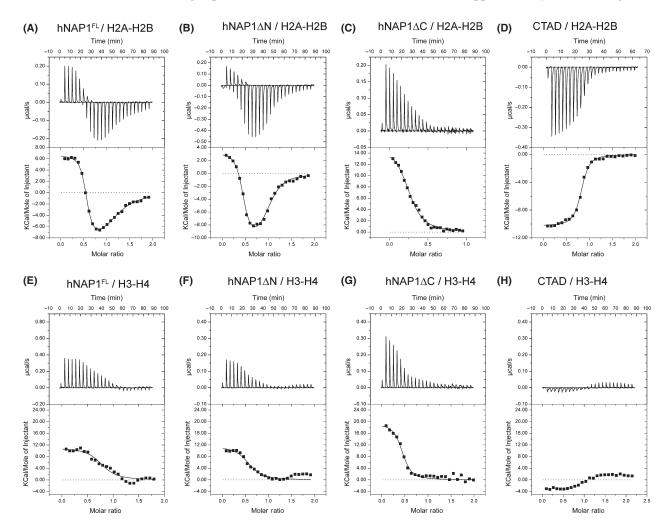

Figure 1 ITC binding curves for the interactions of hNAP1 and its derivatives with H2A-H2B (A–D) and H3-H4 (E–H). (A–H) Top panels show the raw data, and bottom panels show the fitted binding isotherms, as summarized in Table 1.

Table 1 Properties of the interaction between H2A–H2B or H3–H4 and hNAP1 derivatives

Proteins or peptides		Kd (nM)	Error	ΔH (kJ/mol)	Error	$T\Delta S$ (kJ/mol)	ΔG (kJ/mol)
hNAP1[FL] (1–391)/H2A–H2B	Site 1	12.9	2.3	26.2	2.4	70.5	−44.3
	Site 2	1664	971	−42.4	2.1	−10.0	−32.4
hNAP1 ΔN (49–391)/H2A–H2B	Site 1	17.7	4.3	13.8	0.4	57.3	−43.5
	Site 2	1056	373	−53.2	7.6	−19.7	−33.5
hNAP1 ΔC (1–344)/H2A–H2B		283	56.9	72.4	9.4	109.1	−36.7
CTAD (349–381)/H2A–H2B		78.1	21.6	−40.1	2.5	−0.2	−39.9
hNAP1[FL] (1–391)/H3–H4		180	40.3	50.2	7.4	88.0	−37.8
hNAP1 ΔN (49–391)/H3–H4		157	56.6	46.6	2.3	84.8	−38.2
hNAP1 ΔC (1–344)/H3–H4		95.5	31.8	80.8	0.7	120.2	−39.4
CTAD (349–381)/H3–H4		N.D.					

Table 1). Similarly, hNAP1ΔC and hNAP1ΔN bound H3–H4 by a strong endothermic interaction (Fig. 1F,G), suggesting that neither the N- nor C-terminal domain in hNAP1 plays a significant role in binding to H3–H4. In fact, we could not estimate the apparent binding of the isolated CTAD to H3–H4 (Fig. 1H).

hNAP1 dimer binds to single and double H2A–H2B heterodimers

Next, we examined the stoichiometry of binding between hNAP1 proteins (wild type and its deletion mutants) and histones (H2A–H2B and H3–H4) by native MS. In the unbound state, hNAP1 and the deletion mutants showed multimeric binding forms similar to yNAP1 and other NAP1 proteins (Fig. 2, Fig. S2 in Supporting Information) (McBryant & Peersen 2004; Toth *et al.* 2005; Noda *et al.* 2011; Bowman *et al.* 2014). In the presence of one molar equivalent of H2A–H2B heterodimer to each hNAP1 dimer, however, a complex comprising a hNAP1[FL] dimer and a single H2A–H2B heterodimer was observed dominantly, with small peaks corresponding to a dimer of this complex; that is, both complexes observed corresponded to a stoichiometry of one hNAP1 dimer to one H2A–H2B heterodimer. Both hNAP1ΔC and hNAP1ΔN showed similar main peaks corresponding to each mutant hNAP1 dimer bound to a single H2A–H2B heterodimer, but weak signals were observed from complexes corresponding to each mutant tetramer bound to a single H2A–H2B heterodimer, suggesting that the N-terminal and C-terminal domains are likely to inhibit aggregation of the hNAP1 core domain (Fig. 2, Fig. S2 in Supporting Information).

By contrast, in the presence of two molar equivalents of H2A–H2B to each hNAP1 dimer, hNAP1[FL] bound two H2A–H2B heterodimers (Fig. 2), suggesting that hNAP1 has two binding sites for H2A–H2B and that the binding of H2A–H2B to hNAP1 occurs sequentially, whereby a second H2A–H2B heterodimer binds to hNAP1 after the first H2A–H2B has bound. Notably, in the presence of two molar equivalents of H2A–H2B to hNAP1ΔC dimer, the mutant dimer showed binding to one H2A–H2B heterodimer and one H2A–H2B heterodimer plus one monomer (H2A or H2B), in addition to two H2A–H2B heterodimers. This strongly suggests that regarding the two binding sites in hNAP1ΔC, the first binding site is not affected, whereas the second binding site is weakened by the deletion of the CTAD. In addition, the second H2A–H2B heterodimer seemed to be stabilized by the CTAD: In the absence of the CTAD, the second heterodimer appeared partially destabilized, and in some cases, it was dissociated into two monomers, and in the hNAP1ΔC complex, one H2A or H2B monomer was present alongside one heterodimer. We discuss this further below.

In the presence of one molar equivalent of H3–H4, both hNAP1[FL] and hNAP1ΔC bound to a single H3–H4 heterodimer; however, dimers of both complexes were detected in significant amounts as (hNAP1[FL]/H3–H4)₂ and (hNAP1ΔC/H3–H4)₂. This corresponds well with the higher tetramer formation ability of H3–H4 as compared with H2A–H2B (Fig. 2). In the presence of two molar equivalents of H3–H4, both hNAP1[FL] and hNAP1ΔC bound to two H3–H4 heterodimers, suggesting that the H3–H4 binding to hNAP1 is sequential (i.e., the second H3–H4 binds after the first H3–H4 has bound) and neither binding is affected by the CTAD (Fig. 2).
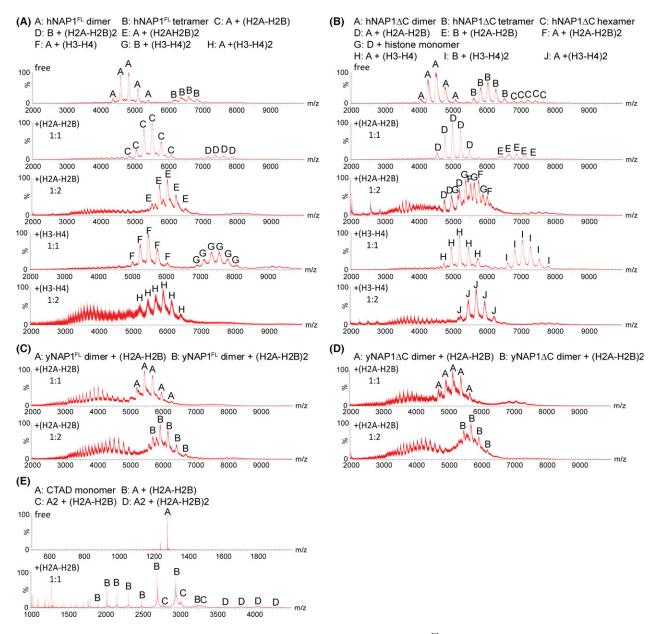
Figure 2 Native ESI mass spectra of NAP1 and histone protein complexes: hNAP1^FL (A) and hNAP1ΔC (B) in the free state and in the presence of H2A–H2B and/or H3–H4. yNAP1^FL (C) and yNAP1ΔC (D) in the presence of H2A–H2B and CTAD in the free state and in the presence of H2A–H2B (E). Proteins were mixed at 1 : 1 or 1 : 2 dimer ratio as indicated. In each figure, A–J show the corresponding mass peaks for their complexes as indicated.

yNAP1 dimer binds to single and double H2A–H2B heterodimers and single and double H3–H4 heterodimers without any contribution of its CTAD

In the presence of one molar equivalent of H2A–H2B, both yNAP1^FL and yNAP1ΔC bound to a single H2A–H2B heterodimer, and in the presence

of two molar equivalents of H2A–H2B, both bound to two H2A–H2B without any detectable effect of the yNAP1 CTAD (Fig. 2). Furthermore, in the presence of one molar equivalent of H3–H4, both yNAP1^FL and yNAP1ΔC bound to a single H3–H4 heterodimer, and in the presence of two molar equivalents of H3–H4, both bound to two

H3–H4, again with no detectable effect of the yNAP1 CTAD (Fig. S3 in Supporting Information). In the case of both H2A–H2B and H3–H4, the binding to yNAP1 seems to be sequential such that the second histone heterodimer binds after the first histone heterodimer; however, two binding sites could not be distinguished, in contrast to hNAP1. According to the previous binding studies of yNAP1 and histone heterodimers (D'Arcy *et al.* 2013), the two binding sites in yNAP1 are likely to be similar symmetrical binding sites in the yNAP1 dimer. The two presumed symmetrical sites may facilitate the binding of histone tetramers, such as (H2A–H2B)$_2$ or (H3–H4)$_2$, in the yNAP1 dimer. Nevertheless, two binding sites were distinguished in hNAP1: Although the CTADs of hNAP1 accelerate binding to H2A–H2B, the stability of the interaction between the first site of hNAP1 and H2A–H2B seems to be independent of the CTADs, but the CTADs assist binding of the second H2A–H2B to the second site of hNAP1 and stabilize this heterodimer against its dissociation into two monomers.

CTAD of hNAP1 has two binding regions for H2A–H2B

In the presence of H2A–H2B, a complex comprising a CTAD monomer and a single H2A–H2B heterodimer was the dominant species, along with very small peaks corresponding to a dimer of this complex and the CTAD dimer bound to a single H2A–H2B heterodimer (Fig. 2). Thus, it is assumed that there are at least two binding regions for CTAD in a single H2A–H2B heterodimer.

Conversely, the isolated CTAD also seems to have two binding regions for H2A–H2B. We investigated the regions in CTAD responsible for binding to H2A–H2B. Two peptides, CTAD-N (amino acids 344–365) and CTAD-C (amino acids 366–387), were prepared, mixed with H2A–H2B and subjected to both native MS and ITC experiments. Figure 3 shows that both CTAD-N and CTAD-C bound strongly to H2A–H2B. Even short two peptide fragments consisting of eight amino acids, F1 in CTAD-N and F5 in CTAD-C, showed a weak but significant binding as summarized in Table 2. In con-
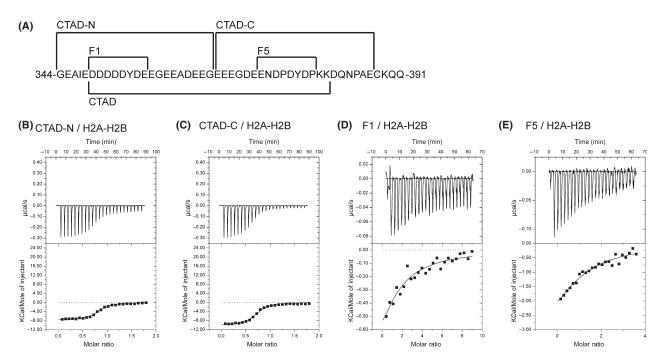

Figure 3 ITC binding curves for the interaction of CTAD derivatives with H2A–H2B. (A) Amino acid sequence of hNAP1 CTAD and its corresponding fragments. (B–E) Top panels show the raw data, and bottom panels show the fitted binding isotherms, as summarized in Table 2. The interactions with H2A–H2B of CTAD-N (amino acids 344–365) (B) and CTAD-C (amino acids 366–387) (C) with H2A–H2B, and of an eight-amino acid fragment in CTAD-N (F1; amino acids 349–356) (D) and in CTAD-C (F5; amino acids 372–379) (E) are shown.

Table 2 Properties of the interaction between H2A–H2B and CTAD derivatives

Proteins or peptides	Kd (nM)	Error	ΔH (kJ/mol)	Error	$T\Delta S$ (kJ/mol)	ΔG (kJ/mol)
CTAD-N (344–365)/H2A–H2B	209	29.5	−32.0	0.5	5.5	−37.5
CTAD-C (366–387)/H2A–H2B	251	40.4	−42.2	0.9	−5.2	−37.0
F1(349–356)/H2A–H2B	31 900	4600	−9.2	0.7	16.0	−25.2
F5(372–379)/H2A–H2B	16 200	566	−20.6	2.3	6.3	−26.9

trast, the two yNAP1 CTADs (amino acids 371–391 and 390–417) did not bind significantly to H2A–H2B as compared with the hNAP1 CTAD by ITC experiments (Fig. S1 in Supporting Information).

In addition, peaks corresponding to a 1 : 1 complex of CTAD-N or CTAD-C peptide of hNAP1 and an H2A–H2B dimer were dominantly observed by native MS (Fig. 4). In the case of CTAD-N, peaks of a 2 : 1 complex of CTAD-N peptide and the H2A–H2B dimer were also observed. Furthermore, weak signals corresponding to a dimer of the 1 : 1 complex were recognized. These results suggest that both the N- and C-terminal regions of CTAD can bind to an H2A–H2B dimer, which is consistent with the ITC results. In the native MS of CTAD with H2A–H2B, as described above, a 1 : 1 complex with the H2A–H2B dimer was dominantly observed, alongside weak signals of a 2 : 1 complex (CTAD: H2A–H2B). Although both the N- and C-terminal regions of CTAD can independently bind to an H2A–H2B dimer, however, a single CTAD peptide of 33 amino acids (349–381 in hNAP1) might not be able to bind to two H2A–H2B dimers simultaneously owing to its small size.

CTAD promotes the nucleosome assembly activity of hNAP1

Above, we showed that the two CTADs in the hNAP1 dimer provide binding assistance for the interaction of hNAP1 with H2A–H2B. In order to

elucidate the role of CTAD in histone chaperone activity, we examined the DNA supercoiling activity of hNAP1^{FL}, hNAP1ΔN, hNAP1ΔC and the isolated CTAD. Each protein was incubated with relaxed circular DNA, in the presence of human histone H2A–H2B and H3–H4 complexes. If the hNAP1 derivatives can properly assemble the histones on the DNA to form nucleosomes, then negative supercoils should be introduced into the DNA. Depending on their concentration, both hNAP1^{FL} and hNAP1ΔN introduced DNA supercoils; however, the DNA supercoiling activity of hNAP1ΔC was greatly reduced as compared with hNAP1^{FL} and hNAP1ΔN (Fig. 5). This further supports our previous finding that the nucleosome assembly activity of an hNAP1 CTAD deletion mutant was slightly decreased. This confirms that both CTADs in the hNAP1 dimer play a significant role in nucleosome assembly, although the isolated CTAD alone had no DNA supercoiling activity even when present in excess quantity (Fig. 5).

Discussion

Native MS showed that the hNAP1 dimer bound sequentially to first and second H2A–H2B heterodimer, and ITC experiments showed two different binding modes: endothermic and exothermic. Although the CTAD deletion mutant of hNAP1 (hNAP1ΔC) showed reduced binding ability to H2A–H2B, it also bound sequentially to two H2A–H2B heterodimers but only by the endothermic
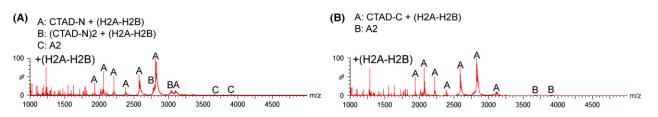

Figure 4 Native ESI mass spectra of hNAP1 CTAD-N (A) and CTAD-C (B) with H2A–H2B. Proteins were mixed at a 1 : 1 ratio of CTAD peptide monomer to H2A–H2B dimer. In each figure, A, B and/or C show the corresponding mass peaks for the complexes as indicated.
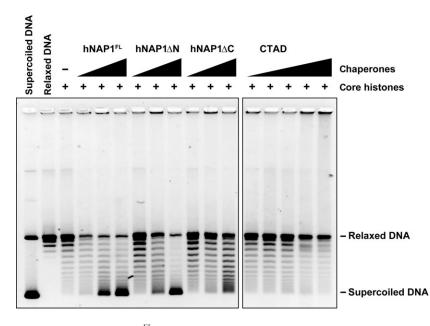
Figure 5 Supercoiling DNA activity of hNAP1^{FL}, hNAP1ΔC, hNAP1ΔN and CTAD. Each amount of 0.25, 0.5 and 1 μM for hNAP1^{FL}, hNAP1ΔC and hNAP1ΔN and of 0.25, 0.5, 1, 5, 10 μM for CTAD was preincubated with H2A-H2B and H3-H4, and then, relaxed DNA was added.

mode. This means that the first and second H2A-H2B binding sites of hNAP1 do not correspond to the endothermic and exothermic binding modes. In addition, native MS showed that the second binding site seemed to be weakened in hNAP1ΔC: That is, a complex between hNAP1ΔC and a single H2A-H2B heterodimer was clearly obtained in the presence of one molar equivalent of H2A-H2B; in the presence of two molar equivalents of H2A-H2B, however, complexes between hNAP1ΔC and one H2A-H2B heterodimer and between hNAP1ΔC and one H2A-H2B heterodimer plus one monomer (H2A or H2B) were identified in addition to the complex between hNAP1ΔC and two H2A-H2B heterodimers. Thus, the second H2A-H2B in the core domain of hNAP1ΔC was not well stabilized and partially dissociated into two monomers, H2A and H2B. In other words, the core domain of the hNAP1 dimer has two binding sites for two H2A-H2B heterodimers; however, the second H2A-H2B binding site requires the assistance of CTADs to stabilize the second H2A-H2B heterodimer within this site. This is in significant contrast to yNAP1, which bound sequentially to a first and then a second H2A-H2B without any help from the CTADs, and in which the first and second binding sites for H2A-H2B were indistinguishable in the present experiments. These findings correspond well to an earlier model showing that the two stable

H2A-H2B heterodimers are symmetrically located in the core domain of yNAP1 (D'Arcy *et al.* 2013). However, that model cannot be applied to the complex between hNAP1 and H2A-H2B.

Here, we modeled the sequential binding of two H2A-H2B heterodimers to hNAP1 as shown in Fig. 6A. In this model, CTAD assists and facilitates binding of the first H2A-H2B heterodimer to the core domain; the first H2A-H2B is quickly transferred to the core domain by CTAD and becomes stably located in the core domain. Next, CTAD assists and facilitates binding of the second H2A-H2B to the core domain; however, binding of the second H2A-H2B is stabilized by both CTAD and the core domain, which cooperatively and dynamically act to retain the second heterodimer. Without CTAD, the core domain still has two binding sites for H2A-H2B; however, it lacks the facilitating activity of CTAD in binding the first and second H2A-H2B heterodimers, and thus, both interactions correspond to the endothermic binding mode of hNAP1ΔC with a Kd value of approximately 300 nM. By contrast, full-length hNAP1 binds strongly to the first and second H2A-H2B heterodimers with endothermic Kd values of approximately 10 nM owing to the facilitating activity of CTAD. In addition, the dynamic equilibrium binding of the second H2A-H2B heterodimer between the core domain and CTAD in full-length hNAP1 seems to correspond to the

exothermic binding mode. This would account for the different Kd values of approximately 10 nM for endothermic binding to the core domain and over 1000 nM for exothermic binding to CTAD in full-length hNAP1. This suggests that CTAD plays a role in transporting both the first and second H2A–H2B heterodimers to the core domain, followed by a role in stabilizing the association of the second H2A–H2B heterodimer. Overall, CTAD provides binding assistance for the interaction of hNAP1 with two H2A–H2B heterodimers; in the process of hNAP1 binding to H3–H4, by contrast, CTAD has no significant role.

We found that CTAD plays a significant role in the supercoiling of DNA mediated by nucleosome assembly of hNAP1. The N-terminal deletion mutant of hNAP1 showed similar supercoiling activity to full-length hNAP1, probably because it has similar H2A–H2B binding activity with the two endothermic and exothermic binding modes. This seems to correspond well to the N-terminal deletion mutant of yNAP1, which shows supercoiling activity similar to that of full-length yNAP1 (McBryant *et al.* 2003). By contrast, the CTAD deletion mutant of hNAP1, hNAP1ΔC, which has greatly reduced ability to bind to H2A–H2B but retains an affinity for H3–H4 similar to that of full-length hNAP1, showed greatly reduced supercoiling activity. However, as compared with the core histone alone,

hNAP1ΔC showed some significant supercoiling bands. Our previous study indicated that in the presence of hNAP1, H3–H4 alone, but not H2A–H2B alone, showed a weak but significant supercoiling activity (Osakabe *et al.* 2010), which may be caused by the formation of a tetrasome by H3–H4. hNAP1ΔC retains H3–H4 binding activity and thus might induce supercoiling of DNA to a similar extent to full-length hNAP1.

Most recently, a study has been published showing that another histone chaperone, FACT, comprising Spt16 and Pob3, binds to H2A–H2B primarily via both of the C-terminal acidic domains of Spt16 and Pob3 (Kemble *et al.* 2015). On the basis of the complex structure between the C-terminal fragment of Spt16 and H2A–H2B, the authors proposed a common binding motif for H2A–H2B in three histone chaperones, FACT (Spt16 and Pob3), Anp32e and Swr1, as shown in Fig. 6B (Kemble *et al.* 2015). Here, we found that the hNAP1 CTAD has two binding regions, which fragmented as F1 and F5 (see Table 2), whose amino acid sequences are well aligned with the H2A–H2B binding motif identified in Spt16, Pob3, Anp32e and Swr1 (Fig. 6B). The proposed motif contains a carboxylic amino acid for capping an H2B helix and an aromatic amino acid for anchoring in hydrophobic pocket of H2B. This suggests that at least one of the binding regions of the
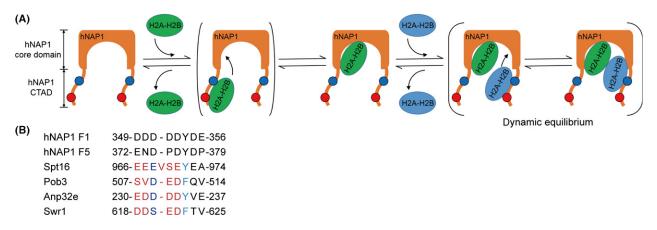

Figure 6 Schematic model of interactions between hNAP1 and H2A–H2B heterodimers. (A) The hNAP1 dimer has two binding sites for H2A–H2B in its core domain and binds sequentially to a first and then a second H2A–H2B assisted by its CTADs. Each CTAD has two binding regions, F1 and F5, for H2A–H2B as indicated in blue and red, respectively. The first H2A–H2B stably binds to a binding site within the core domain; this interaction is accelerated by CTAD. The second H2A–H2B binds to a binding site comprising both the core domain and CTAD; in this interaction, CTAD plays a significant role in both accelerating the binding and stabilizing the second H2A–H2B heterodimer in hNAP1. (B) Amino acid sequences of the two regions of the hNAP1 CTAD (F1 and F5) that are responsible for H2A–H2B binding aligned with the proposed H2A–H2B binding motif in Spt16 and Pob3 of FACT, Anp32e and Swr1 (Kemble *et al.* 2015). In each motif, the capping amino acid and the anchoring amino acid are colored dark and light blue, respectively, and the other amino acids are colored red.

hNAP1 CTAD binds to H2A–H2B in a manner similar to the C-terminal acidic domain of Spt16. However, the two regions in the hNAP1 CTAD bind to a single H2A–H2B; thus, they seem to bind to two different regions of the same H2A–H2B heterodimer. At least one of two regions must bind to H2A–H2B in a manner different from that of the proposed motif; however, the details of this await investigation in future experiments.

Experimental procedures

Purification of hNAP1 and its deletion mutants

Purification of hNAP1^{FL} (1–391 amino acids), hNAP1ΔN (49–391 amino acids) and hNAP1ΔC (1–344 amino acids) was carried out by similar method as described previously (Tachiwana *et al.* 2008). hNAP1 and its deletion mutants were bacterially expressed as His$_6$ tag fusion proteins in Rosetta-gami B (DE3) cells. Proteins were purified by HisTrap HP (GE Healthcare), and the His$_6$ tag was cleaved with Turbo3C protease (Accelagen). Proteins without the His$_6$ tag were then purified by a Q Sepharose (GE Healthcare) column. The eluted samples were run through a Superdex 200 (GE Healthcare) column and were finally purified by the Q Sepharose column again. Purified hNAP1 and its deletion mutants were dialyzed against 20 mM Tris–HCl (pH 7.5) buffer, containing 150 mM NaCl, 1 mM DTT, 0.5 mM EDTA, 0.1 mM PMSF and 10% glycerol.

Purification of yNAP1 and its CTAD deletion mutant

yNAP1 (amino acids 1–417) and its CTAD deletion mutant (amino acids 1–365) were purified by method similar to that for hNAP1. The proteins were bacterially expressed in Rosetta-gami B (DE3) cells as His$_6$ tag fusion proteins and were purified by an Ni-NTA agarose column. Next, the His$_6$ tag was cleaved with thrombin protease (GE Healthcare), and the proteins were purified by a MonoQ (GE Healthcare) column. The eluted samples were passed through a Superdex 200 column and finally purified by passage through the MonoQ column again. Purified yNAP1 and its CTAD deletion mutants were dialyzed against 20 mM Tris–HCl (pH 7.5) buffer, containing 150 mM NaCl, 1 mM DTT, 0.5 mM EDTA, 0.1 mM PMSF and 10% glycerol.

CTAD and its derivatives

Peptides corresponding to CTAD (amino acids 349–381), CTAD-N (amino acids 344–365), CTAD-C (amino acids 366–387), F1 (amino acids 349–356), F5 (amino acids 372–379) of hNAP1 and two yNAP1 CTADs (amino acids 371–391 and 390–417) were synthesized by SIGMA Genosys.

Purification of H2A and H2B

Recombinant human H2A and H2B were prepared according to the previously published method (Tanaka *et al.* 2004). We modified an existing pET-23b-based vector, which encodes an N-terminal oct-histidine (His8) tag, and Turbo3C protease cleavage site followed by Lumio^{TM} tag (Invitrogen). Proteins were expressed in *Escherichia coli* strain BL21 (DE3) star grown in LB medium.

The harvested cells were resuspended in buffer A (50 mM Tris pH 8.0, 500 mM NaCl), lysed on ice by sonication and centrifuged. The pellet was solubilized in buffer B (50 mM Tris pH 8.0, 500 mM NaCl, 7 M guanidine hydrochloride). The protein solution was then applied to an immobilized metal affinity chromatography (IMAC) column (Bio-Rad) equilibrated with buffer B, and His-tagged H2A or H2B was eluted by buffer C (50 mM Tris–HCl pH 8.0, 500 mM NaCl, 3 M guanidine hydrochloride and 300 mM imidazole). The eluted His-tagged H2A or H2B was dialyzed against buffer D (20 mM Tris pH 8.0 and 5 mM mercaptoethanol) and digested with Turbo3C protease (Accelagen) at 4 °C overnight. The protein solution was again loaded onto the IMAC column. Fractions passing through the column were concentrated and dialyzed against pure water. Finally, the purified H2A or H2B was lyophilized.

Lyophilized H2A and H2B were mixed at a molar ratio of 1 : 1, and H2A–H2B dimer was refolded by dialysis first against buffer E (20 mM Tris pH 8.0, 1 mM ethylene diamine tetraacetic acid (EDTA) and 2 M NaCl) and then against buffer F (20 mM Tris pH 8.0, 1 mM EDTA and 1 M NaCl) at 4 °C. After dialysis, the sample solution was subjected to size-exclusion chromatography using a column of Superdex 200 pg (GE Healthcare) equilibrated with buffer F at 4 °C, and fractions containing H2A–H2B dimer were collected.

Purification of H3–H4 complex

Purification of the H3-H4 tetramer was carried out as described previously (Osakabe *et al.* 2013). Freeze-dried H3 and H4 proteins were mixed at 1 : 1 molar ratio under denaturing buffer. Next, the H3-H4 complex was refolded by dialysis and purified by Superdex 200 gel filtration chromatography with 20 mM Tris–HCl (pH 7.5) buffer, containing 100 mM NaCl, 1 mM EDTA, 1 mM PMSF, 5% glycerol and 5 mM 2-mercaptoethanol.

Isothermal titration calorimetry (ITC) experiments

Protein solutions at 5–10 μM protein in buffer (25 mM MES pH 6.0 with 200 mM KCl) were loaded into a cell (active volume 1.4 mL) in a VP-ITC isothermal titration calorimeter (Microcal, Inc.). Each protein solution was titrated using a 300-μL titration syringe against 100–500 μM ligand solution prepared in the same buffer. Experiments were carried out at 20 °C. All titration experiments were repeated at least twice.

H Ohtomo *et al.*

The heat of dilution generated by ligands was subtracted, and the binding isotherms were fitted to a one-site or two-site binding model using ORIGIN 7 Software (Microcal, Inc.). From the values of Kd and ΔH, the thermodynamic parameters ΔG and ΔS were calculated according to the basic thermodynamic equations:

$$\Delta G = -RT \ln Kd^{-1} \tag{1}$$

$$\Delta G = \Delta H - T\Delta S \tag{2}$$

Native mass spectrometry

Native mass spectrometry was carried out on Synapt G2 HDMS instruments (Waters, Milford, MA, USA) as previously reported (Saikusa *et al.* 2013). Before MS analysis, protein samples were dialyzed against 200 mM ammonium acetate and the sample concentration was adjusted to ~5 μM. An aliquot of protein solution was deposited in a nanoESI spray tip (HUMANIX, Japan) and placed in the nanoESI spray source. Ions were generated with the capillary voltage of 0.75–1 kV.

Supercoiling assay

The supercoiling assay was carried out as described previously (Kato *et al.* 2015). The indicated amount of hNAP1 was preincubated with H2A-H2B (0.4 μM) and H3-H4 (0.4 μM) at 37 °C for 15 min, and the relaxed DNA (100 ng) was then added to the reaction mixture (10 μL) in 10 mM Tris–HCl (pH 7.5) buffer, containing 140 mM NaCl, 5 mM DTT and 2.2 mM MgCl2. The reaction was continued at 37 °C for 60 min and then stopped by the addition of stop solution [20 mM Tris–HCl (pH 8.0), 20 mM EDTA, 0.25% SDS and 0.5 mg/mL proteinase K (Roche)]. The samples were further incubated at 37 °C for 15 min. The DNA samples were then extracted by phenol–chloroform and analyzed by 1% agarose gel electrophoresis in 1× TAE (40 mM Tris–acetate and 1 mM EDTA) with SYBR Gold staining (Invitrogen).

References

Akey, C.W. & Luger, K. (2003) Histone chaperones and nucleosome assembly. *Curr. Opin. Struct. Biol.* **13**, 6–14.

Andrews, A.J., Chen, X., Zevin, A., Stargell, L.A. & Luger, K. (2010) The histone chaperone Nap1 promotes nucleosome assembly by eliminating nonnucleosomal histone DNA interactions. *Mol. Cell* **37**, 834–842.

Andrews, A.J., Downing, G., Brown, K., Park, Y.J. & Luger, K. (2008) A thermodynamic model for Nap1-histone interactions. *J. Biol. Chem.* **283**, 32412–32418.

Asahara, H., Tartare-Deckert, S., Nakagawa, T., Ikehara, T., Hirose, F., Hunter, T., Ito, T. & Montminy, M. (2002) Dual roles of p300 in chromatin assembly and transcriptional activation in cooperation with nucleosome assembly protein 1 *in vitro*. *Mol. Cell. Biol.* **22**, 2974–2983.

Attia, M., Förster, A., Rachez, C., Freemont, P., Avner, P. & Rogner, U.C. (2011) Interaction between nucleosome assembly protein 1-like family members. *J. Mol. Biol.* **407**, 647–660.

Azegami, N., Saikusa, K., Todokoro, Y., Nagadoi, A., Kurumizaka, H., Nishimura, Y. & Akashi, S. (2013) Conclusive evidence of the reconstituted hexasome proven by native mass spectrometry. *Biochemistry* **52**, 5155–5157.

Benesch, J.L., Ruotolo, B.T., Simmons, D.A. & Robinson, C.V. (2007) Protein complexes in the gas phase: technology for structural genomics and proteomics. *Chem. Rev.* **107**, 3544–3567.

Bowman, A., Hammond, C.M., Stirling, A., Ward, R., Shang, W., El-Mkami, H., Robinson, D.A., Svergun, D.I., Norman, D.G. & Owen-Hughes, T. (2014) The histone chaperones Vps75 and Nap1 form ring-like, tetrameric structures in solution. *Nucleic Acids Res.* **42**, 6038–6051.

D'Arcy, S., Martin, K.W., Panchenko, T., Chen, X., Bergeron, S., Stargell, L.A., Black, B.E. & Luger, K. (2013) Chaperone Nap1 shields histone surfaces used in a nucleosome and can put H2A-H2B in an unconventional tetrameric form. *Mol. Cell* **51**, 662–677.

De Koning, L., Corpet, A., Haber, J.E. & Almouzni, G. (2007) Histone chaperones: an escort network regulating histone traffic. *Nat. Struct. Mol. Biol.* **14**, 997–1007.

Eitoku, M., Sato, L., Senda, T. & Horikoshi, M. (2008) Histone chaperones: 30 years from isolation to elucidation of the mechanisms of nucleosome assembly and disassembly. *Cell. Mol. Life Sci.* **65**, 414–444.

Fujii-Nakata, T., Ishimi, Y., Okuda, A. & Kikuchi, A. (1992) Functional analysis of nucleosome assembly protein, NAP-1. The negatively charged COOH-terminal region is not necessary for the intrinsic assembly activity. *J. Biol. Chem.* **267**, 20980–20986.

Heck, A.J. (2008) Native mass spectrometry: a bridge between interactomics and structural biology. *Nat. Methods* **5**, 927–933.

Ishimi, Y., Hirosumi, J., Sato, W., Sugasawa, K., Yokota, S., Hanaoka, F. & Yamada, M. (1984) Purification and initial characterization of a protein which facilitates assembly of nucleosome-like structure from mammalian cells. *Eur. J. Biochem.* **142**, 431–439.

Ito, T., Ikehara, T., Nakagawa, T., Kraus, W.L. & Muramatsu, M. (2000) p300-mediated acetylation facilitates the transfer of histone H2A-H2B dimers from nucleosomes to a histone chaperone. *Genes Dev.* **14**, 1899–1907.

Kato, D., Osakabe, A., Tachiwana, H., Tanaka, H. & Kurumizaka, H. (2015) Human tNASP promotes *in vitro* nucleosome assembly with histone H3.3. *Biochemistry* **54**, 1171–1179.

Kemble, D.J., McCullough, L.L., Whitby, F.G., Formosa, T. & Hill, C.P. (2015) FACT disrupts nucleosome structure by binding H2A-H2B with conserved peptide motifs. *Mol. Cell* **60**, 294–306.

Kimura, H., Takizawa, N., Allemand, E., Hori, T., Iborra, F.J., Nozaki, N., Muraki, M., Hagiwara, M., Krainer, A.R., Fukagawa, T. & Okawa, K. (2006) A novel histone exchange factor, protein phosphatase 2Cgamma, mediates the exchange and dephosphorylation of H2A-H2B. *J. Cell Biol.* **175**, 389–400.

Lorch, Y., Maier-Davis, B. & Kornberg, R.D. (2006) Chromatin remodeling by nucleosome disassembly *in vitro*. *Proc. Natl Acad. Sci. USA* **103**, 3090–3093.

Luebben, W.R., Sharma, N. & Nyborg, J.K. (2010) Nucleosome eviction and activated transcription require p300 acetylation of histone H3 lysine 14. *Proc. Natl Acad. Sci. USA* **107**, 19254–19259.

Luger, K. (2003) Structure and dynamic behavior of nucleosomes. *Curr. Opin. Genet. Dev.* **13**, 127–135.

McBryant, S.J., Park, Y.J., Abernathy, S.M., Laybourn, P.J., Nyborg, J.K. & Luger, K. (2003) Preferential binding of the histone (H3-H4)2 tetramer by NAP1 is mediated by the amino-terminal histone tails. *J. Biol. Chem.* **278**, 44574–44583.

McBryant, S.J. & Peersen, O.B. (2004) Self-association of the yeast nucleosome assembly protein 1. *Biochemistry* **43**, 10592–10599.

Mizuguchi, G., Shen, X., Landry, J., Wu, W.H., Sen, S. & Wu, C. (2004) ATP-driven exchange of histone H2AZ variant catalyzed by SWR1 chromatin remodeling complex. *Science* **303**, 343–348.

Newman, E.R., Kneale, G.G., Ravelli, R.B., Karuppasamy, M., Karimi Nejadasl, F., Taylor, I.A. & McGeehan, J.E. (2012) Large multimeric assemblies of nucleosome assembly protein and histones revealed by small-angle X-ray scattering and electron microscopy. *J. Biol. Chem.* **287**, 26657–26665.

Noda, M., Uchiyama, S., McKay, A.R., Morimoto, A., Misawa, S., Yoshida, A., Shimahara, H., Takinowaki, H., Nakamura, S., Kobayashi, Y., Matsunaga, S., Ohkubo, T., Robinson, C.V. & Fukui, K. (2011) Assembly states of the nucleosome assembly protein 1 (NAP-1) revealed by sedimentation velocity and non-denaturing MS. *Biochem. J.* **436**, 101–112.

Okuwaki, M., Kato, K. & Nagata, K. (2010) Functional characterization of human nucleosome assembly protein 1-like proteins as histone chaperones. *Genes Cells* **15**, 13–27.

Osakabe, A., Tachiwana, H., Matsunaga, T., Shiga, T., Nozawa, R.S., Obuse, C. & Kurumizaka, H. (2010) Nucleosome formation activity of human somatic nuclear autoantigenic sperm protein (sNASP). *J. Biol. Chem.* **285**, 11913–11921.

Osakabe, A., Tachiwana, H., Takaku, M., Hori, T., Obuse, C., Kimura, H., Fukagawa, T. & Kurumizaka, H. (2013) Vertebrate Spt2 is a novel nucleolar histone chaperone that assists in ribosomal DNA transcription. *J. Cell Sci.* **126**, 1323–1332.

Park, Y.J., Chodaparambil, J.V., Bao, Y., McBryant, S.J. & Luger, K. (2005) Nucleosome assembly protein 1 exchanges histone H2A-H2B dimers and assists nucleosome sliding. *J. Biol. Chem.* **280**, 1817–1825.

Park, Y.J. & Luger, K. (2006) The structure of nucleosome assembly protein 1. *Proc. Natl Acad. Sci. USA* **103**, 1248–1253.

Saikusa, K., Kuwabara, N., Kokabu, Y., Inoue, Y., Sato, M., Iwasaki, H., Shimizu, T., Ikeguchi, M. & Akashi, S. (2013) Characterisation of an intrinsically disordered protein complex of Swi5-Sfr1 by ion mobility mass spectrometry and small-angle X-ray scattering. *Analyst* **138**, 1441–1449.

Shikama, N., Chan, H.M., Krstic-Demonacos, M., Smith, L., Lee, C.W., Cairns, W. & La Thangue, N.B. (2000) Functional interaction between nucleosome assembly proteins and p300/CREB-binding protein family coactivators. *Mol. Cell. Biol.* **20**, 8933–8943.

Tachiwana, H., Osakabe, A., Kimura, H. & Kurumizaka, H. (2008) Nucleosome formation with the testis-specific histone H3 variant, H3t, by human nucleosome assembly proteins *in vitro*. *Nucleic Acid Res.* **36**, 2208–2218.

Tanaka, Y., Tawaramoto-Sasanuma, M., Kawaguchi, S., Ohta, T., Yoda, K., Kurumizaka, H. & Yokoyama, S. (2004) Expression and purification of recombinant human histones. *Methods* **33**, 3–11.

Toth, K.F., Mazurkiewicz, J. & Rippe, K. (2005) Association states of nucleosome assembly protein 1 and its complexes with histones. *J. Biol. Chem.* **280**, 15690–15699.

Supporting Information

Additional supporting information might/can be found in the supporting information tab for this article:

Figure S1 ITC binding curves for the interactions of yNAP1^{FL} and its derivatives with H2A-H2B (A–D), and the interaction of yNAP1^{FL} with H3-H4 (E).

Figure S2 Native ESI mass spectra of hNAP1ΔN in the absence (upper) and presence (lower) of H2A-H2B (A) and hNAP1^{FL} with H2A-H2B (B).

Figure S3 Native ESI mass spectra of yNAP1^{FL} with H3-H4 (A) and yNAP1ΔC with H3-H4 (B).

Table S1 Properties of the interaction between H2A–H2B or H3-H4 and yNAP1 derivatives